Equilibrium climate sensitivity estimated by equilibrating climate models

Maria Rugenstein, Jonah Bloch-johnson, Jonathan Gregory, Timothy Andrews, Thorsten Mauritsen, Chao Li, Thomas L. Frölicher, David Paynter, Gokhan Danabasoglu, Shuting Yang, et al.

Equilibrium climate sensitivity estimated by equilibrating climate models

Maria Rugenstein[1,2*], Jonah Bloch-Johnson[3], Jonathan Gregory[3,4], Timothy Andrews[4], Thorsten Mauritsen[5], Chao Li[1], Thomas Frölicher[6,7], David Paynter[8], Gokhan Danabasoglu[9], Shuting Yang[10], Jean-Louis Dufresne[11], Long Cao[12], Gavin A. Schmidt[13], Ayako Abe-Ouchi[14], Olivier Geoffroy[15], and Reto Knutti[2]

[1]Max-Planck-Institute for Meteorology, Bundestrasse 53, 20146 Hamburg, Germany
[2]Institute for Atmospheric and Climate Science, ETH Zurich, CH-8092 Zurich, Switzerland
[3]NCAS-climate, University of Reading, Reading
[4]UK Met Office Hadley Centre, FitzRoy Road, Exeter, EX1 3PB
[5]Stockholm University, SE-106 91 Stockholm, Sweden
[6]Climate and Environmental Physics, Physics Institute, University of Bern, Switzerland
[7]Oeschger Centre for Climate Change Research, University of Bern, Switzerland
[8]Geophysical Fluid Dynamics Laboratory, Princeton, New Jersey, USA
[9]National Center for Atmospheric Research, P.O. Box 3000, Boulder, CO 80307
[10]Danish Meteorological Institute, Lyngbyvej 100, DK-2100 Copenhagen, Denmark
[11]Centre National de la Recherche Scientifique, Universit Pierre et Marie Curie, ENS, Ecole Polytechnique, Paris, France
[12]School of Earth Sciences, Zhejiang University, Hang Zhou, Zhejiang Province, 310027, China
[13]NASA Goddard Institute for Space Studies, 2880 Broadway, New York, NY 10025
[14]Center for Climate System Research, The University of Tokyo, Japan
[15]CNRM, Université de Toulouse, Météo-France, CNRS, Toulouse, France

Key Points:

- 27 simulations of 15 general circulation models are integrated to near equilibrium
- All models develop a higher equilibrium climate sensitivity than predicted by extrapolating methods
- The tropics and Southern Hemisphere mid latitudes dominate the change of the global feedback parameter

*Max-Planck-Institute for Meteorology, Bundestrasse 53, 20146 Hamburg, Germany

Corresponding author: Maria Rugenstein, maria.rugenstein@mpimet.mpg.de

Abstract

The global mean equilibrium warming is higher than expected from extrapolating transient time scales in our new collection of millennial long general circulation models. 27 simulations with 15 general circulation models from 10 modeling centers show a 5-53% (median 15%) larger equilibrium climate sensitivity (ECS) than estimated by the "Gregory" method. The spatial patterns of radiative feedbacks change continuously, becoming less stable in most regions. However, in the equatorial Pacific, initially positive feedbacks decrease, thus, become more stabilizing with equilibration time. The global feedback evolution is initially dominated by the tropics, but joined eventually by the Southern Hemisphere mid latitudes. Time-dependent feedbacks underscore the need to define a measure of climate sensitivity which ensures different models, observations, and paleo proxies are similarly equilibrated when compared to each other and combined to estimate future warming.

1 Estimating equilibrium climate sensitivity

The equilibrium climate sensitivity (ECS) is defined as the annual-mean, global-mean, surface air warming once radiative equilibrium is reached in response to doubling the atmospheric CO_2 concentration above pre-industrial levels. It is by far the most commonly and continuously used concept to assess our understanding of the climate system expressed in climate models and it is used to compare models, observations, and paleo-proxies (Knutti et al., 2017; Charney, 1979). Due to the large heat capacity of the ocean, the climate system takes millennia to equilibrate to a forcing perturbation, but simulating such a long equilibration time with a climate model is computationally expensive. As a result, many modeling studies use extrapolation methods on short, typically 150-year long, simulations to project equilibrium conditions (Taylor et al., 2011; Andrews et al., 2012; Collins et al., 2013; Otto et al., 2013; Lewis & Curry, 2015; Andrews et al., 2015; Forster, 2016; Calel & Stainforth, 2017). These so-called *effective* climate sensitivities (Murphy, 1995; Gregory et al., 2004) are often reported as ECS values (Hargreaves & Annan, 2016; Tian, 2015; Brient & Schneider, 2016; Forster, 2016). Recent research provides evidence for decadal-to-centennial changes of feedbacks (Murphy, 1995; Senior & Mitchell, 2000; Gregory et al., 2004; Winton et al., 2010; Armour et al., 2013; Proistosescu & Huybers, 2017) but the behavior on longer timescales has not been compared among models. Here, we utilize LongRunMIP, a large set of millennia-long coupled general circulations models (GCMs) to estimate the true

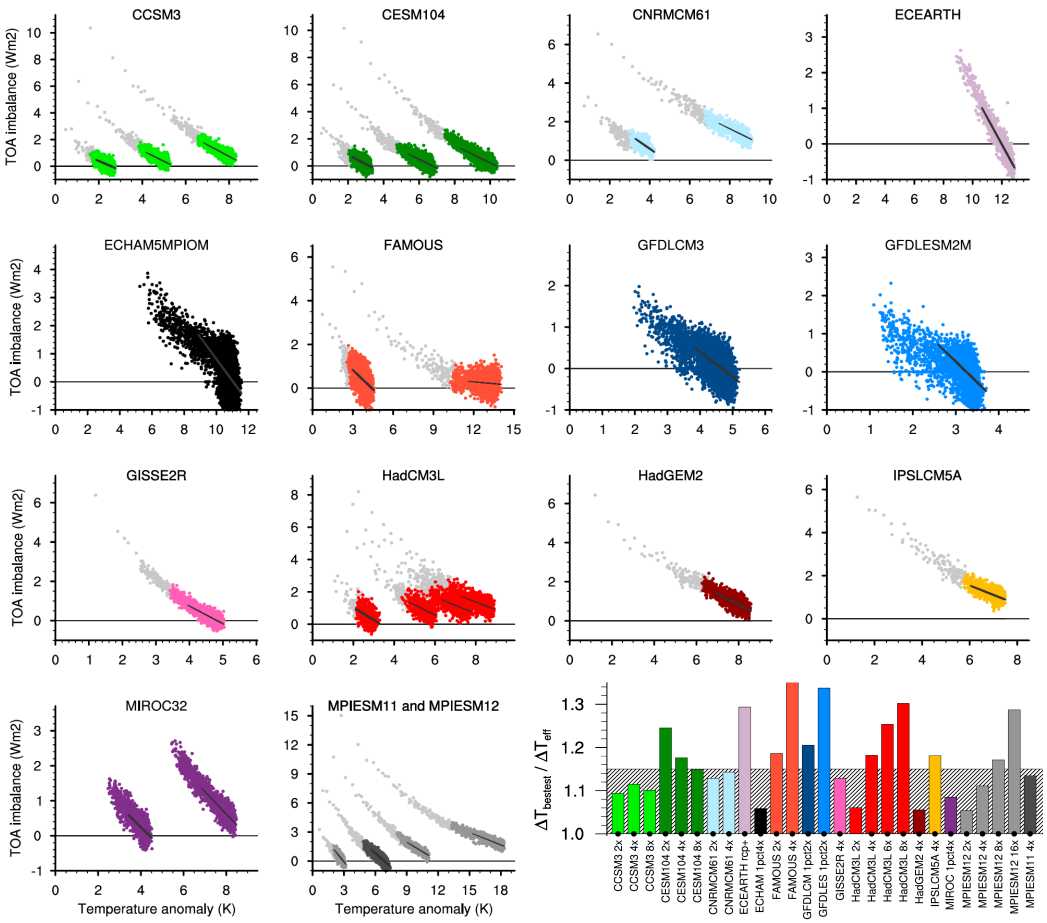

Figure 1. Evolution of global and annual mean top of the atmosphere (TOA) imbalance and surface temperature anomalies for simulations contributing to LongRunMIP (14 small panels). The first 150 years of step forcing simulations are depicted in gray. For experiments which are not step forcing simulations only the period after stabilizing CO_2 concentrations is shown. The black line shows the linear regression of TOA imbalance and surface warming for the last 15% of warming. The panel on the lower right shows the ratio $\Delta\,\mathrm{T}_{\mathrm{best\,est}}/\Delta\mathrm{T}_{\mathrm{eff}\,1-150}$, see text for definitions. A dot at the lower end of the bar indicates that the 90% confidence intervals of $\Delta\,\mathrm{T}_{\mathrm{best\,est}}$ and $\Delta\mathrm{T}_{\mathrm{eff}\,1-150}$ obtained by resampling 10'000 times do not overlap. The gray hashed bar in the background is the median of all simulations. FAMOUS *abrupt4x* is outside of the depicted range at 1.53. SM Table 1 specifies the model versions and names, length of simulations, and numerical values for different climate sensitivity estimates.

equilibrium climate sensitivity, study the centennial-to-millennial behavior of the climate system under elevated radiative forcing, and test extrapolation methods. LongRunMIP is a model intercomparison project (MIP) that is opportunistic in that we collect millennial long simulations withouth a previously agreed upon protocol. The minimum contribution is a simulation of at least 1000 years with a constant CO_2 forcing level. It consists mostly out of doubling or quadrupling step forcing simulations ("abrupt2x", "abrupt4x", ...) as well as increases in CO_2 achieved through annual increments of 1% reaching doubled or quadrupled concentrations ("1pct2x", "1pct4x"; Fig. 1). SM Table 1 lists the simulations and models used in this paper, Rugenstein et al. (subm.) documents the modeling effort and more contributions in detail.

The equilibration of top of the atmosphere (TOA) radiative imbalance and surface temperature anomaly of the simulations are depicted in Fig. 1. Throughout the manuscript, we show anomalies as the difference to the mean of the unforced control simulation. Gray dots indicate annual means of the first 150 years of a step forcing simulation, requested by the protocol of CMIP5 (Eyring et al., 2016) and widely used to infer ECS (Andrews et al., 2012; Geoffroy, Saint-Martin, Olivié, et al., 2013). We refer to this time scale as "decadal to centennial". Colors indicate the LongRunMIP gain, the "centennial to millennial" time scales we explore here. The distance to the reference line at TOA = 0 indicates that most simulations are close to equilibrium, however, even if a simulation equilibrated the TOA imbalance, the surface temperature, surface heat fluxes, or ocean temperatures can still show a trend (discussed in Rugenstein et al. (subm.)). We define the best estimate of equilibrium warming, $\Delta\,\mathrm{T}_{\mathrm{best\,est}}$, as the temperature-axis intersect of the regression of annual means in TOA imbalance and surface temperature anomaly over the simulation's final 15% of global mean warming (black lines in Fig. 1). We use "Δ T" instead of "ECS" to indicate that we study equilibration for a range of forcing levels, not *abrupt2x* only. Other simulations can be scaled to match the ECS definition (values given in SM Table 1). The lower right panel in Fig. 1 illustrates that all simulations eventually warm significantly more (measured by $\Delta\,\mathrm{T}_{\mathrm{best\,est}}$) then predicted by the most commonly used method to estimate the equilibrium temperature by extrapolating a least-square regression of the first 150 years (Gregory et al., 2004; Flato et al., 2013), denoted here "$\Delta\,\mathrm{T}_{\mathrm{eff\,1-150}}$". While this method implies a constant feedback parameter – the slope of the regression line – other extrapolation methods allow for a time dependent feedback parameter, but usually fail to predict $\Delta\,\mathrm{T}_{\mathrm{best\,est}}$ by estimating too low values (up to 28%) and for some models too high values (up to 16%).

Linearly regressing year 20-150 results in a too low model median ECS of 7%, while the two layer energy balance model including ocean heat uptake efficacy results in a too low model median ECS of 9% (see discussion around SM Fig. 1 and SM Table 1 for a description of the extrapolation methods). The results are qualitatively the same if $\Delta\,T_{\mathrm{best\,est}}$ is defined by regressing regressions over the last 20 instead of 15% of warming or without using TOA imbalance information but instead time averaging the surface warming toward the end of every simulation.

2 Global feedback evolution

Current extrapolation methods underestimate the equilibrium response because climate feedbacks change with the degree of equilibration (Murphy, 1995; Senior & Mitchell, 2000; Andrews et al., 2015; Knutti & Rugenstein, 2015; Rugenstein, Caldeira, & Knutti, 2016; Armour, 2017; Proistosescu & Huybers, 2017; Paynter et al., 2018). We define the global net TOA feedback as the *local tangent* in temperature-TOA space (dTOA/dT) computed by a least square regression of all global and annual means of netTOA imbalance and surface temperature anomaly within a temperature bin, which is moved in steps of 0.1 K throughout the temperature space to obtain the continuous local slope of the point cloud (sketched out in SM Fig. 2a and described in Rugenstein, Gregory, et al. (2016)). We decompose the net TOA imbalance into its clear sky and cloud radiative effects (CRE; Soden and Held (2006); Ceppi and Gregory (2017)) in the shortwave and longwave (Fig. 2 a). The feedbacks do not change on obviously separable time scales, but continuously – in some models more at the beginning of the simulations (Fig. 2 a1), in some models after 150 years (Fig. 2 a3) or, in some models, intermittently throughout the simulation (Fig. 2 a2, a4). The shortwave CRE dominates the magnitude and the timing of the net feedback change, and can be counteracted by the longwave CRE (Fig. 2a1, a2). The reduction of the shortwave clear sky feedback associated with ice albedo, lapse rate, and water vapor is a function of temperature and occurs on centennial to millennial time scales. Longwave clear sky changes, when present, contribute to a small increase of the sensitivity with equilibration time and temperature. The net feedback parameter can be composed of a subtle balance of different components at any time (Fig. 2a2, a4) and the forced signal is not obviously linked to the feedback arising from internal variability (circles in Fig. 2a), defined by regressing all available annual and global means of TOA imbalance and surface temperature anomalies (relative to the mean) of the control simulations.

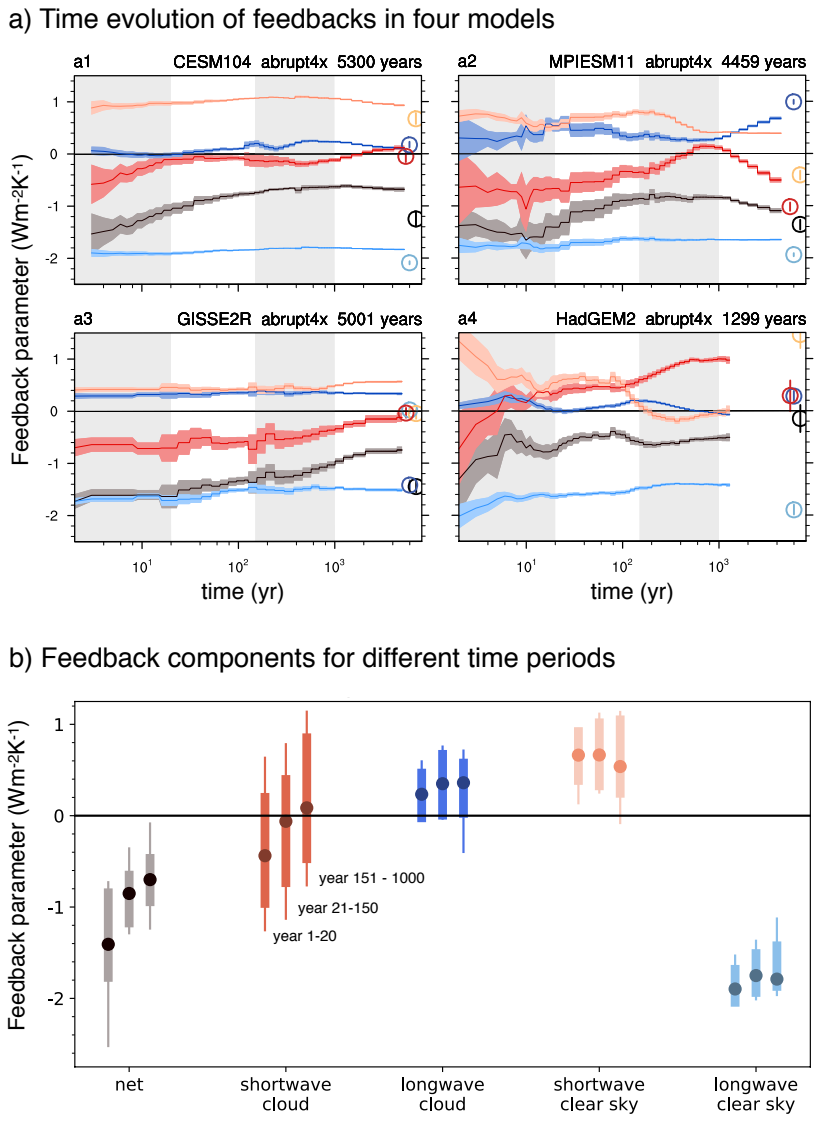

Figure 2. Time evolution of global feedbacks (a) Continuous feedback evolution for four characteristic models. Net TOA feedback (gray) is the sum of its components: the cloud effects in the shortwave (red) and longwave (blue), and clear sky feedbacks in the shortwave (salmon) and longwave (light blue). Circles at the right of each panel indicate the feedbacks arising from internal variability; shading and vertical lines shows the 2.5-97.5% confidence intervals. Panel titles give the model name and length of the simulation. Time periods of 1-20 years and 150-1000 years are shaded gray. (b) Feedback evolution in all available simulations of all models for three time periods. Dots represent median values, bars spans all but the two highest and lowest simulations, and the line spans all simulations. SM Fig. 4 and 5 show panel a and b for all simulations.

Models which are more sensitive at the beginning of the simulation are generally also more sensitive towards the end of the equilibration, however, the feedback factor can chance little or up to an order of magnitude. We can quantify the continuous changes across models by considering different time periods, e.g., years 1-20, 21-150, and 151-1000 (Fig. 2b), for which we regress all points within these time periods. In addition to the increase of the feedback parameter between year 1-20 and 21-150, which is documented for CMIP5 models (Geoffroy, Saint-Martin, Bellon, et al., 2013; Andrews et al., 2015; Proistosescu & Huybers, 2017; Ceppi & Gregory, 2017), there is a further increase on centennial to millennial timescales. The model spread is large and does not substantially reduce in time.

Previous research has shown that the change in feedbacks over time can come about through a dependence of feedback processes on the increasing temperature (Hansen et al., 1984; Jonko et al., 2013; Caballero & Huber, 2013; Meraner et al., 2013; Bloch-Johnson et al., 2015), due to evolving surface warming patterns and feedback processes (Senior & Mitchell, 2000; Winton et al., 2010; Armour et al., 2013; Rugenstein, Gregory, et al., 2016; Gregory & Andrews, 2016; Paynter et al., 2018), or both. Though we will focus in the following on robust pattern changes in surface temperatures and feedbacks, which occur in most or all simulations irrespective of their overall temperature anomaly, we analyze temperature dependence for the six models which contributed more than one forcing level. $\Delta T_{\text{best est}}$ calculated from the abrupt4x forcing is somewhat larger than from the abrupt2x forcing (SM Table 1; Jonko et al. (2013); Block and Mauritsen (2013); Gregory et al. (2015); Good et al. (2015)), however the relation between the forcing levels also changes with equilibration time in most models (not shown). This means the relation between ECS estimates calculated from *abrupt2x* and *abrupt4x* simulations depends on the method and definition of the sensitivity measure.

3 Pattern evolution of surface warming and feedbacks

The evolution of surface warming patterns during the three time periods discussed above displays a fast establishment of a land-sea warming contrast, Arctic amplification, and the delayed warming over the Southern Ocean that have been studied on decadal to centennial time scales (Fig. 3; Senior and Mitchell (2000); Li et al. (2013); Collins et al. (2013); Armour et al. (2016)). Arctic amplification does not change substantially, whereas Antarctic amplification strengthens approximately 50% on centennial to millennial timescales (Salzmann, 2017; Rugenstein et al., subm.). The warming in the North Atlantic reflects the initial

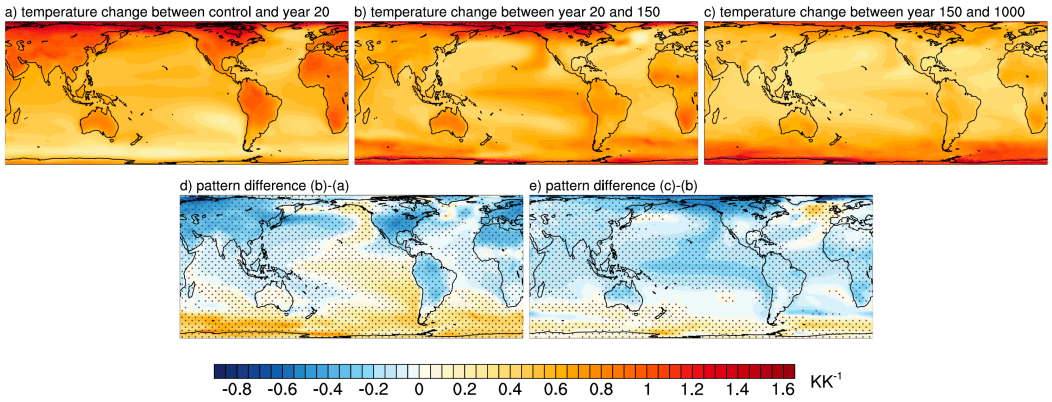

Figure 3. Model-mean normalized patterns of surface warming (local warming divided by global warming) between the average of (a) the control simulation and year 15-25, (b) year 15-25 and 140-160, (c) year 140-160 and 900-1000, and their differences (d and e). Only the models CCSM3, CESM104, CNRMCM6, ECHAM5MPIOM, FAMOUS, GISSE2R, HadCM3L, HadGEM2, IPSLCM5A, MPIESM11, and MPIESM12 are used with their step forcing simulations. For models contributing several simulations, these are averaged. Stippling in panel d and e indicates that 9 out of 11 models agree in sign.

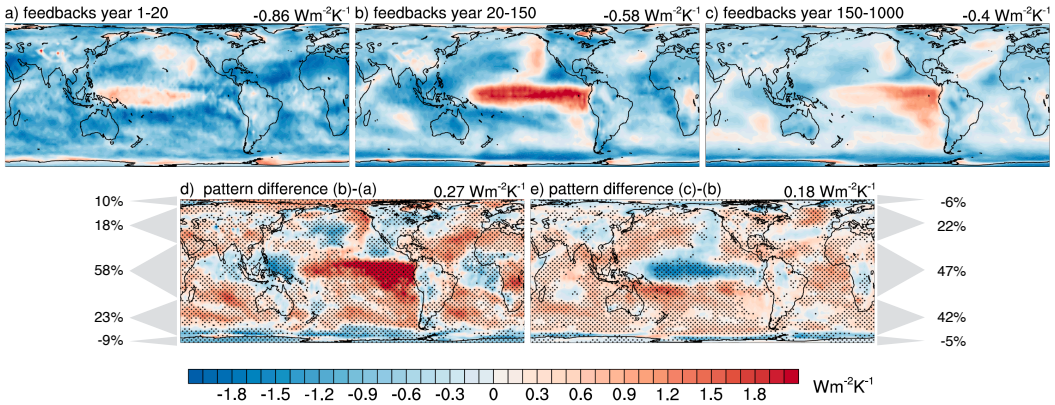

Figure 4. Time evolution of feedback patterns. Model-mean of local contribution to the change in global feedbacks (local TOA anomaly divided by global warming during the period indicated in the panel titles; see text for definitions) (a–c) and their differences (d, e). The global feedback value is shown in the panel title. Regionally aggregated contributions to the global values are indicated with gray triangles (22°S-22°N, 22°S/N-66°S/N, 66°S/N-90°S/N, representing 40%, 27%, and 4% of the global surface area respectively) and percent numbers. Model selection, weighting, and stippling is the same as in Fig. 3. SM Fig. 6–12 shows all TOA components.

decline and subsequent strengthening of the Atlantic Meridional Overturning Circulation (Stouffer & Manabe, 2003; Li et al., 2013; Rind et al., 2018; Jansen et al., 2018). In the Pacific, at all times, the warm pool temperatures stay warmer than the East Pacific in absolute terms in all but two models (not shown). The equatorial east Pacific warms more than the warm pool in all but three simulations, a phenomenon reminiscent of the positive phase of the El-Niño-Southern-Oscillation (ENSO) or the Interdecadal Pacific Oscillation (IPO) ("ENSO-like warming" (Song & Zhang, 2014; Andrews et al., 2015; Luo et al., 2017)). Through time, this tendency first increases (Fig. 3d) but then stays constant or reverses sign (Fig. 3e), meaning that the East and West equatorial Pacific warm at the same rate or not at all. Robustly, across all simulations, the difference between the South East Pacific and warm pool temperatures increase, with the warm pool initially warming more, but later less than the South East Pacific, with the inflection point occurring as early as the first decade and as later as 3000 years. While the reduction of the walker circulation coincides with the decadal to centennial ENSO-like warming pattern, it does not correspond to changes on the centennial to millennial time scales, indicating that subtropical gyre advection and upwelling play a more prominent role on the longer time scales (Knutson & Manabe, 1995; Song & Zhang, 2014; Andrews & Webb, 2018; Luo et al., 2017; Zhou et al., 2017).

Feedbacks defined as the local tangent in temperature-TOA space as used in Fig. 2 contain a signal from both the internal variability and the forced response. In order to isolate the forced response, we take the difference of the means at the beginning and end of the time periods discussed above. We call this definition of feedbacks *finite difference approach*, as it represents a change *across* a time period; SM Fig. 2b. Fig. 4 shows the local contribution to the global net TOA changes for the same time periods and models as used in Fig. 3. In the initial years, the atmosphere restores radiative balance through increased radiation to space almost everywhere, except in the western-central Pacific (Fig. 4a), whereas on decadal to centennial time scales, the structure of the feedbacks mirrors the surface temperature evolution and develops a pattern reminiscent of ENSO/IPO (Fig. 4b). The cloud response dominates this pattern SM Fig. 6-8, which is attributed for CMIP5 models to the lapse rate and cloud feedbacks (Andrews et al., 2015; Andrews & Webb, 2018; Ceppi & Gregory, 2017). For the millennial time scales, our models show that feedbacks become less negative almost everywhere, switching from slightly negative to positive in parts of the Southern Ocean and North Atlantic region, and become less destabilizing in the Tropical Pacific (Fig. 4c). Unexpectedly, the feedback pattern change from decadal to centennial time scales (Fig. 4d)

is reversed in many regions on the centennial to millennial time scales (Fig. 4e), namely in the entire Pacific basin, the Atlantic, and parts of Asia and North America. This "pattern flip" is dominated by longwave CRE (SM Fig. 8) and mirrors the reduction in ENSO/IPO-like surface warming patterns discussed for the surface temperature evolution. Although the spatial patterns of changing temperature and radiative feedbacks vary a lot among models, the large scale features discussed here occur robustly across most models and forcing levels, and also occur in the *ramp* simulations.

4 Regional accounting for changing global feedbacks

We quantify the contribution of different regions to the global feedback change (% numbers in Fig. 4d,e). Whereas the tropics account for the bulk of the change (58% on decadal to centennial and 47% on centennial to millennial time scales), the mid-latitudes become more important with time (Northern and Souther Hemisphere combined 41% on decadal to centennial and 66% on centennial to millennial time scales). The high latitudes, dominated by the shortwave clear sky feedback (SM Fig. 12), play only a minor role in influencing the global response at all timescales. This regional accounting of global feedbacks permits us to test competing explanations regarding the spatial feedback pattern by placing them in a common temporal framework (Senior & Mitchell, 2000; Li et al., 2013; Jonko et al., 2013; Caballero & Huber, 2013; Paynter et al., 2018). The Southern Hemispheric mid to high latitudes (Senior & Mitchell, 2000), the Northern Hemispheric subpolar regions (Rose & Rayborn, 2016; Trossman et al., 2016), and the Tropics (Jonko et al., 2013; Meraner et al., 2013; Block & Mauritsen, 2013; Andrews et al., 2015), especially in the Pacific (Andrews & Webb, 2018; Ceppi & Gregory, 2017) have all been suggested to be the primary region controlling the global feedback evolution. Our models show a delayed Southern relative to Northern Hemispheric warming throughout the millennia-long simulations, which correlates with the time evolution of net TOA and shortwave CRE (not shown), confirming the hypothesis of Senior and Mitchell (2000). The subtropical cloud response in the model-mean is non-negligible in the Southern Ocean and North Atlantic on decadal to centennial time scales as proposed by Rose et al. 2016 and Trossman et al. 2016; however, it comes to dominate the global response only on centennial to millennial time scales. We find that the longwave clear sky feedback does moderately increase in many models as the temperature or the forcing level increases, mainly in the tropics and Northern Hemispheric mid-latitudes (Fig. 2a and SM Fig. 3 and 4). This is in accordance with the proposed argument that the

tropics govern the global feedback evolution because the water vapor feedback increases with warming (Jonko et al., 2013; Meraner et al., 2013; Block & Mauritsen, 2013; Andrews et al., 2015), following the rising tropical tropopause (Meraner et al., 2013). The importance of the Pacific response and the regions of short and longwave cloud response (SM Fig. 6–8) in our models qualitatively agree with the proposed change of tropospheric stability patterns on decadal to centennial time scales (Andrews & Webb, 2018; Ceppi & Gregory, 2017). However, on centennial to millennial time scales, the Pacific response becomes less important compared to the mid-latitudes and the net tropical CRE becomes negligible (SM Fig. 6).

5 Implications

We demonstrate that, though the feedback response in the first century is dominated by the tropics, the mid-latitudes come to lead the global feedback response in subsequent centuries. We stress that the global net feedback change is a result of a subtle balance of a) different regions and b) different TOA components at all times (even more so in single simulations than in than in the model mean shown here (Rugenstein, Caldeira, & Knutti, 2016; Paynter et al., 2018; Andrews & Webb, 2018)). This underscores the necessity of process-based feedback studies in individual models as well as multi-model ensembles to draw robust conclusions. It may be difficult to compare the observed regional responses and time scales with GCM behavior (Ceppi & Gregory, 2017); however, the similarity of unforced (SM Fig. 3) and forced (Fig. 4d) feedbacks in the tropics indicates that it may be possible to connect feedbacks in the near future and feedbacks inferred from the satellite record. Ways forward to relate the model's forced response to the observational record include (1) increasing our theoretical understanding of formation of surface temperature patterns, the interaction of tropospheric stability, clouds, and surface temperature, (2) increasing our understanding of model biases, especially the ocean-atmosphere interactions, and (3) studying how observed historical trends and paleoclimate data constrain the various climate and Earth system sensitivities discussed here.

Our results show that sensitivity tends to increase over millennia on the approach to equilibrium. ECS has been historically used as a model benchmark (Charney, 1979), but give the strong time dependence of radiative feedbacks, one might argue that the transient climate response (TCR) or the effective climate sensitivity (here called $\Delta T_{\mathrm{eff}\,1-150}$) might be better measures to characterize e.g., the next few decades to centuries (Knutti et al.,

2017). However, next to being not an accurate indicator of the equilibrium response, these alternative climate sensitivity measures capture the models in different degrees of equilibration (Fig. 1). Part of the spread in these sensitivities among models might be due to different degrees of equilibration (different SST patterns) and not per se different feedback magnitudes. These climate sensitivity measures also capture different degrees of internal variability for each model (Fig. 2 and SM Fig. 2). It has been recently shown that ECS correlates higher than TCR with the end-of-21st-century warming across models (Gregory et al., 2015; Grose et al., 2018) and it is an open question how TCR, ECS, and the effective climate sensitivity relate to each other (Fig. 1 and SM Fig. 1; see also e.g., Knutti et al. (2015) or Millar et al. (2015)). ECS estimates based on paleo-proxies usually assume equilibrated "fast" feedbacks, which we show are changing on millennial time scales. Thus, we underscore the need of defining a new, clear, measure of climate sensitivity, which ensures different models, observations, and paleo proxies are in the same state when compared to each other or combined in calculations to estimate future warming.

Acknowledgments

LongRunMIP data is available to download `ftp://longrunmip:password_available_upon_request@data.iac.ethz.ch`. See `www.longrunmip.org` and Rugenstein et al. (subm.) for more details. We thank Urs Beyerle, Erich Fischer, Jeremy Rugenstein, Levi Silvers, and Martin Stolpe for technical help and comments on the manuscript.

NCAR is sponsored by the US National Science Foundation.

References

Andrews, T., Gregory, J. M., & Webb, M. J. (2015). The dependence of radiative forcing and feedback on evolving patterns of surface temperature change in climate models. *Journal of Climate*, *28*(4), 1630-1648. Retrieved from `http://dx.doi.org/10.1175/JCLI-D-14-00545.1`

Andrews, T., Gregory, J. M., Webb, M. J., & Taylor, K. E. (2012). Forcing, feedbacks and climate sensitivity in CMIP5 coupled atmosphere-ocean climate models. *Geophysical Research Letters*, *39*(9). Retrieved from `http://dx.doi.org/10.1029/2012GL051607`

Andrews, T., & Webb, M. J. (2018). The Dependence of Global Cloud and Lapse Rate Feedbacks on the Spatial Structure of Tropical Pacific Warming. *Journal of Climate*, *31*(2), 641-654. Retrieved from `https://doi.org/10.1175/JCLI-D-17-0087.1` doi:

10.1175/JCLI-D-17-0087.1

Armour, K. C. (2017, 04 17). Energy budget constraints on climate sensitivity in light of inconstant climate feedbacks. *Nature Climate Change*, *7*, 331 EP -. Retrieved from http://dx.doi.org/10.1038/nclimate3278

Armour, K. C., Bitz, C. M., & Roe, G. H. (2013). Time-Varying Climate Sensitivity from Regional Feedbacks. *Journal of Climate*, *26*(13), 4518–4534. Retrieved from http://dx.doi.org/10.1175/JCLI-D-12-00544.1

Armour, K. C., Marshall, J., Scott, J. R., Donohoe, A., & Newsom, E. R. (2016, 07). Southern ocean warming delayed by circumpolar upwelling and equatorward transport. *Nature Geosci*, *9*(7), 549–554. Retrieved from http://dx.doi.org/10.1038/ngeo2731

Bloch-Johnson, J., Pierrehumbert, R. T., & Abbot, D. S. (2015). Feedback temperature dependence determines the risk of high warming. *Geophysical Research Letters*, *42*(12), 4973– 4980. Retrieved from http://dx.doi.org/10.1002/2015GL064240 (2015GL064240) doi: 10.1002/2015GL064240

Block, K., & Mauritsen, T. (2013). Forcing and feedback in the MPI-ESM-LR coupled model under abruptly quadrupled CO_2. *Journal of Advances in Modeling Earth Systems*, *5*(4), 676–691. Retrieved from http://dx.doi.org/10.1002/jame.20041

Brient, F., & Schneider, T. (2016). Constraints on Climate Sensitivity from Space-Based Measurements of Low-Cloud Reflection. *Journal of Climate*, *29*(16), 5821-5835. Retrieved from https://doi.org/10.1175/JCLI-D-15-0897.1 doi: 10.1175/JCLI-D-15-0897.1

Caballero, R., & Huber, M. (2013). State-dependent climate sensitivity in past warm climates and its implications for future climate projections. *Proceedings of the National Academy of Sciences of the United States of America*, *110*(35), 14162–14167. Retrieved from http://www.ncbi.nlm.nih.gov/pmc/articles/PMC3761583/

Calel, R., & Stainforth, D. A. (2017). On the Physics of Three Integrated Assessment Models. *Bulletin of the American Meteorological Society*, *98*(6), 1199-1216. Retrieved from https://doi.org/10.1175/BAMS-D-16-0034.1 doi: 10.1175/BAMS-D-16-0034.1

Ceppi, P., & Gregory, J. M. (2017). Relationship of tropospheric stability to climate sensitivity and earth's observed radiation budget. *Proceedings of the National Academy of Sciences*, *114*(50), 13126–13131. Retrieved from https://www.pnas.org/content/114/50/13126 doi: 10.1073/pnas.1714308114

Charney, J. (1979). *Carbon Dioxide and Climate: A Scientific Assessment* (Tech. Rep.). Washington, DC..

Collins, M., Knutti, R., Arblaster, J. M., Dufresne, J.-L., Fichefet, T., Friedlingstein, P., ... Wehner, M. F. (2013). Long-term Climate Change: Projections, Commitments and Irreversibility. In T. Stocker et al. (Eds.), *Climate Change 2013: The Physical Science Basis. Contribution of Working Group I to the Fifth Assessment Report of the Intergovernmental Panel on Climate Change.* Cambridge University Press.

Eyring, V., Bony, S., Meehl, G. A., Senior, C. A., Stevens, B., Stouffer, R. J., & Taylor, K. E. (2016). Overview of the Coupled Model Intercomparison Project Phase 6 (CMIP6) experimental design and organization. *Geoscientific Model Development*, *9*(5), 1937–1958. Retrieved from https://www.geosci-model-dev.net/9/1937/2016/ doi: 10.5194/gmd-9-1937-2016

Flato, G., Marotzke, J., Abiodun, B., Braconnot, P., Chou, S., Collins, W., ... Rummukainen, M. (2013). Evaluation of Climate Models. In T. Stocker et al. (Eds.), *Climate Change 2013: The Physical Science Basis. Contribution of Working Group I to the Fifth Assessment Report of the Intergovernmental Panel on Climate Change.* Cambridge University Press, Cambridge, United Kingdom and New York, NY, USA.

Forster, P. M. (2016). Inference of climate sensitivity from analysis of earth's energy budget. *Annual Review of Earth and Planetary Sciences*, *44*(1), 85-106. Retrieved from http://dx.doi.org/10.1146/annurev-earth-060614-105156 doi: 10.1146/annurev-earth-060614-105156

Geoffroy, O., Saint-Martin, D., Bellon, G., Voldoire, A., Olivié, D., & Tytéca, S. (2013). Transient Climate Response in a Two-Layer Energy-Balance Model. Part II: Representation of the Efficacy of Deep-Ocean Heat Uptake and Validation for CMIP5 AOGCMs. *Journal of Climate*, *26*(6), 1859–1876. Retrieved from http://dx.doi.org/10.1175/JCLI-D-12-00196.1

Geoffroy, O., Saint-Martin, D., Olivié, D. J. L., Voldoire, A., Bellon, G., & Tytéca, S. (2013). Transient Climate Response in a Two-Layer Energy-Balance Model. Part I: Analytical Solution and Parameter Calibration Using CMIP5 AOGCM Experiments. *Journal of Climate*, *26*(6), 1841–1857. Retrieved from http://dx.doi.org/10.1175/JCLI-D-12-00195.1

Good, P., Lowe, J. A., Andrews, T., Wiltshire, A., Chadwick, R., Ridley, J. K., ... Shiogama, H. (2015, 02). Nonlinear regional warming with increasing co2 concentrations.

Nature Clim. Change, *5*(2), 138–142. Retrieved from http://dx.doi.org/10.1038/nclimate2498

Gregory, J. M., & Andrews, T. (2016). Variation in climate sensitivity and feedback parameters during the historical period. *Geophysical Research Letters*, *43*(8), 3911–3920. Retrieved from http://dx.doi.org/10.1002/2016GL068406

Gregory, J. M., Andrews, T., & Good, P. (2015). The inconstancy of the transient climate response parameter under increasing CO_2. *Philosophical Transactions of the Royal Society of London A: Mathematical, Physical and Engineering Sciences*, *373*(2054). Retrieved from http://rsta.royalsocietypublishing.org/content/373/2054/20140417

Gregory, J. M., Ingram, W. J., Palmer, M. A., Jones, G. S., Stott, P. A., Thorpe, R. B., ... Williams, K. D. (2004). A new method for diagnosing radiative forcing and climate sensitivity. *Geophysical Research Letters*, *31*(3). Retrieved from http://dx.doi.org/10.1029/2003GL018747

Grose, M. R., Gregory, J., Colman, R., & Andrews, T. (2018). What Climate Sensitivity Index Is Most Useful for Projections? *Geophysical Research Letters*, *45*(3), 1559–1566. Retrieved from http://dx.doi.org/10.1002/2017GL075742 doi: 10.1002/2017GL075742

Hansen, J., Lacis, A., Rind, D., Russel, G., Stone, P., Fung, I., ... Lerner, J. (1984). Analysis of feedback mechanisms. In: Climate processes and climate sensitivity. In J. Hansen & T. Takahashi (Eds.), *Climate sensitivity: Analysis of feedback mechanisms* (Vol. 5, pp. 130–163). American Geophysical Union, Washington, DC: AGU Geophysical Monograph 29, Maurice Ewing.

Hargreaves, J. C., & Annan, J. D. (2016). Could the pliocene constrain the equilibrium climate sensitivity? *Climate of the Past*, *12*(8), 1591–1599. Retrieved from http://www.clim-past.net/12/1591/2016/ doi: 10.5194/cp-12-1591-2016

Jansen, M. F., Nadeau, L.-P., & Merlis, T. M. (2018). Transient versus Equilibrium Response of the Ocean's Overturning Circulation to Warming. *Journal of Climate*, *31*(13), 5147-5163. Retrieved from https://doi.org/10.1175/JCLI-D-17-0797.1 doi: 10.1175/JCLI-D-17-0797.1

Jonko, A. K., Shell, K. M., Sanderson, B. M., & Danabasoglu, G. (2013). Climate Feedbacks in CCSM3 under Changing CO2 Forcing. Part II: Variation of Climate Feedbacks and Sensitivity with Forcing. *Journal of Climate*, *26*(9), 2784-2795. Retrieved from

http://dx.doi.org/10.1175/JCLI-D-12-00479.1

Knutson, T. R., & Manabe, S. (1995). Time-Mean Response over the Tropical Pacific to Increased $C0_2$ in a Coupled Ocean-Atmosphere Model. *Journal of Climate*, *8*(9), 2181-2199. Retrieved from https://doi.org/10.1175/1520-0442(1995)008<2181:TMROTT>2.0.CO;2 doi: 10.1175/1520-0442(1995)008⟨2181:TMROTT⟩2.0.CO;2

Knutti, R., Rogelj, J., Sedláček, J., & Fischer, E. M. (2015, 12 07). A scientific critique of the two-degree climate change target. *Nature Geoscience*, *9*, 13 EP -. Retrieved from http://dx.doi.org/10.1038/ngeo2595

Knutti, R., & Rugenstein, M. A. A. (2015). Feedbacks, climate sensitivity and the limits of linear models. *Philosophical Transactions of the Royal Society of London A: Mathematical, Physical and Engineering Sciences*, *373*(2054). doi: 10.1098/rsta.2015.0146

Knutti, R., Rugenstein, M. A. A., & Hegerl, G. C. (2017, 09 04). Beyond equilibrium climate sensitivity. *Nature Geoscience*, *10*, 727 EP -. Retrieved from http://dx.doi.org/10.1038/ngeo3017

Lewis, N., & Curry, J. A. (2015). The implications for climate sensitivity of AR5 forcing and heat uptake estimates. *Climate Dynamics*, *45*(3), 1009–1023. Retrieved from http://dx.doi.org/10.1007/s00382-014-2342-y

Li, C., Storch, J.-S., & Marotzke, J. (2013). Deep-ocean heat uptake and equilibrium climate response. *Climate Dynamics*, *40*(5-6), 1071-1086. Retrieved from http://dx.doi.org/10.1007/s00382-012-1350-z

Luo, Y., Lu, J., Liu, F., & Garuba, O. (2017). The Role of Ocean Dynamical Thermostat in Delaying the El Niño–Like Response over the Equatorial Pacific to Climate Warming. *Journal of Climate*, *30*(8), 2811-2827. Retrieved from https://doi.org/10.1175/JCLI-D-16-0454.1 doi: 10.1175/JCLI-D-16-0454.1

Meraner, K., Mauritsen, T., & Voigt, A. (2013). Robust increase in equilibrium climate sensitivity under global warming. *Geophysical Research Letters*, *40*(22), 5944–5948. Retrieved from http://dx.doi.org/10.1002/2013GL058118

Millar, R. J., Otto, A., Forster, P. M., Lowe, J. A., Ingram, W. J., & Allen, M. R. (2015, Jul 01). Model structure in observational constraints on transient climate response. *Climatic Change*, *131*(2), 199–211. Retrieved from https://doi.org/10.1007/s10584-015-1384-4 doi: 10.1007/s10584-015-1384-4

Murphy, J. M. (1995, 2014/06/21). Transient Response of the Hadley Centre Coupled Ocean-Atmosphere Model to Increasing Carbon Dioxide. Part 1: Control Climate

and Flux Adjustment. *Journal of Climate*, *8*(1), 36–56. Retrieved from http://dx.doi.org/10.1175/1520-0442(1995)008<0036:TROTHC>2.0.CO;2

Otto, A., Otto, F. E. L., Boucher, O., Church, J., Hegerl, G., Forster, P. M., ... Allen, M. R. (2013, 06). Energy budget constraints on climate response. *Nature Geosci*, *6*(6), 415–416. Retrieved from http://dx.doi.org/10.1038/ngeo1836

Paynter, D., Frölicher, T. L., Horowitz, L. W., & Silvers, L. G. (2018). Equilibrium Climate Sensitivity Obtained From Multimillennial Runs of Two GFDL Climate Models. *Journal of Geophysical Research: Atmospheres*, *123*(4), 1921-1941. Retrieved from https://agupubs.onlinelibrary.wiley.com/doi/abs/10.1002/2017JD027885 doi: 10.1002/2017JD027885

Proistosescu, C., & Huybers, P. J. (2017). Slow climate mode reconciles historical and model-based estimates of climate sensitivity. *Science Advances*, *3*(7). Retrieved from http://advances.sciencemag.org/content/3/7/e1602821 doi: 10.1126/sciadv.1602821

Rind, D., Schmidt, G. A., Jonas, J., Miller, R., Nazarenko, L., Kelley, M., & Romanski, J. (2018). Multicentury Instability of the Atlantic Meridional Circulation in Rapid Warming Simulations With GISS ModelE2. *Journal of Geophysical Research: Atmospheres*, *123*(12), 6331-6355. Retrieved from https://agupubs.onlinelibrary.wiley.com/doi/abs/10.1029/2017JD027149 doi: 10.1029/2017JD027149

Rose, B. E. J., & Rayborn, L. (2016). The Effects of Ocean Heat Uptake on Transient Climate Sensitivity. *Current Climate Change Reports*, 1–12. Retrieved from http://dx.doi.org/10.1007/s40641-016-0048-4

Rugenstein, M. A. A., Bloch-Johnson, J., Abe-Ouchi, A., Andrews, T., Beyerle, U., Cao, L., ... Yang, S. (subm.). LongRunMIP – motivation, design and data access for a large collection of millennial long AO-GCM simulations. *subm. to BAMS*.

Rugenstein, M. A. A., Caldeira, K., & Knutti, R. (2016). Dependence of global radiative feedbacks on evolving patterns of surface heat fluxes. *Geophysical Research Letters*, *43*(18), 9877–9885. Retrieved from http://dx.doi.org/10.1002/2016GL070907

Rugenstein, M. A. A., Gregory, J. M., Schaller, N., Sedláček, J., & Knutti, R. (2016). Multiannual Ocean–Atmosphere Adjustments to Radiative Forcing. *Journal of Climate*, *29*(15), 5643-5659. Retrieved from http://dx.doi.org/10.1175/JCLI-D-16-0312.1

Salzmann, M. (2017). The polar amplification asymmetry: role of Antarctic surface height.

Earth System Dynamics, *8*(2), 323–336. Retrieved from https://www.earth-syst-dynam.net/8/323/2017/ doi: 10.5194/esd-8-323-2017

Senior, C. A., & Mitchell, J. F. B. (2000). The time-dependence of climate sensitivity. *Geophysical Research Letters*, *27*(17), 2685–2688. Retrieved from http://dx.doi.org/10.1029/2000GL011373

Soden, B. J., & Held, I. M. (2006). An Assessment of Climate Feedbacks in Coupled Ocean-Atmosphere Models. *Journal of Climate*, *19*(14), 3354-3360. Retrieved from http://dx.doi.org/10.1175/JCLI3799.1

Song, X., & Zhang, G. J. (2014, 2014/07/26). Role of Climate Feedback in El Nino-like SST Response to Global Warming. *Journal of Climate*. Retrieved from http://dx.doi.org/10.1175/JCLI-D-14-00072.1 doi: 10.1175/JCLI-D-14-00072.1

Stouffer, R., & Manabe, S. (2003). Equilibrium response of thermohaline circulation to large changes in atmospheric CO_2 concentration. *Climate Dynamics*, *20*(7-8), 759-773. Retrieved from http://dx.doi.org/10.1007/s00382-002-0302-4

Taylor, K. E., Stouffer, R. J., & Meehl, G. A. (2011, 2013/11/05). An Overview of CMIP5 and the Experiment Design. *Bulletin of the American Meteorological Society*, *93*(4), 485–498. Retrieved from http://dx.doi.org/10.1175/BAMS-D-11-00094.1 doi: 10.1175/BAMS-D-11-00094.1

Tian, B. (2015). Spread of model climate sensitivity linked to double-intertropical convergence zone bias. *Geophysical Research Letters*, *42*(10), 4133–4141. Retrieved from http://dx.doi.org/10.1002/2015GL064119 doi: 10.1002/2015GL064119

Trossman, D. S., Palter, J. B., Merlis, T. M., Huang, Y., & Xia, Y. (2016). Large-scale ocean circulation-cloud interactions reduce the pace of transient climate change. *Geophysical Research Letters*, *43*(8), 3935–3943. Retrieved from http://dx.doi.org/10.1002/2016GL067931

Winton, M., Takahashi, K., & Held, I. M. (2010). Importance of Ocean Heat Uptake Efficacy to Transient Climate Change. *Journal of Climate*, *23*(9), 2333-2344. Retrieved from http://dx.doi.org/10.1175/2009JCLI3139.1 doi: 10.1175/2009JCLI3139.1

Zhou, C., Zelinka, M. D., & Klein, S. A. (2017). Analyzing the dependence of global cloud feedback on the spatial pattern of sea surface temperature change with a green's function approach. *Journal of Advances in Modeling Earth Systems*, *9*(5), 2174–2189. Retrieved from http://dx.doi.org/10.1002/2017MS001096 doi: 10.1002/2017MS001096